rate $\sqrt{N}$. Based on this decomposition, we arrive at the follow results about the convergence of factor estimation error.

Theorem 4 (Factor Estimation Asymptotics)**.**
Under Assumptions A–F, with an identification Θ *that satisfies IF.1–2,*
(4.a) *Factor estimation is consistent: as* $N, T \to \infty$, $\widehat{f}_t(\widehat{\Gamma}) - \widetilde{f}_t\left(\Gamma^0(\Theta)\right) \xrightarrow{p} \mathbf{0}$.
(4.b) *Factor estimation error centered against the normalized true factor converges to a normal distribution at the rate of* $\sqrt{N}$*: as* $N, T \to \infty$, $\forall t$,

$$\sqrt{N}\left(\widehat{f}_t(\widehat{\Gamma}) - \widetilde{f}_t\left(\Gamma^0(\Theta)\right)\right) \xrightarrow{d} \text{Normal}\left(\mathbf{0}, \mathbb{V}_t^{[2]}\right).^{34}$$

The theorem gives the factor's asymptotic distribution under a generic normalization Θ. Similar to Γ estimation, we can evaluate $\mathbb{V}_t^{[2]}$ at either the $\Gamma^0(\Theta_{\text{X}})$ or $\Gamma^0(\Theta_{\text{Y}}^0)$ normalizations.[35]

7 Simulations

This section presents a concise set of simulations that illustrate the behavior of the IPCA estimation in finite samples, and assess the accuracy of approximation based on the asymptotic theory derived above. To summarize, we find that estimation errors are well-approximated with a normal distribution. This is true even in rather small samples, and when the true generating process has errors with large variance. This shows that applied researchers can confidently assume normality for confidence intervals and hypothesis tests when applying IPCA, as it verifies the asymptotic derivations in the previous section. We present details below.

For given N, T, we generate a stochastic panel of c, f^0, e and use these to assemble the x panel. We calibrate the simulated data to the IPCA model (fixing $K = 2$ and $L = 10$) estimated from US monthly stock returns in KPS.[36]

Simulations proceed according to the following steps:

[34] The expression of the asymptotic variance $\mathbb{V}_t^{[2]}$ is with the proof in Appendix C.14.

[35] Appendix B.3 contains the asymptotics when centered by the original f_t^0. This situation corresponds to Arrow C for Γ estimation, and the the additional stochastic wedge introduced by a sample-based normalization affects the asymptotic distribution.

[36] In particular, we use the ten most significant instruments from KPS as calibration targets. They are market capitalization, total assets, market beta, short-term reversal, momentum, turnover, price relative to its 52-week high, long-term reversal, unexplained volume, and idiosyncratic volatility with respect to the Fama-French three factor model.

1. **Generate factors**. Fit a VAR(1) process to estimated IPCA factors from KPS. Simulate f_t^0 according to the estimated VAR employing normal innovations.

2. **Generate instruments**. For each stock, calculate the time-series averages of the instruments. Pool the demeaned characteristics into a panel and estimate a ten variable panel VAR(1). Next, for each i, generate the means of $c_{i,t}$ as an i.i.d. draw from the empirical distribution of the time series means. Then, simulate the dynamic component of $c_{i,t}$ from the estimated VAR with normal innovations.[37]

3. **Generate errors**. Elements of the error panel e are simulated from an i.i.d. normal distribution whose variance is calibrated so that the population R^2, defined as $1-\mathbb{E}e^2/\mathbb{E}x^2$, equals 20%, matching the empirical R^2 in the estimated model in KPS.

4. **Generate main panel**. We fix $\widehat{\Gamma}(\Theta_{\text{Y}})$ at its empirically estimated value and calculate $x_{i,t}$ according to model equation (3).

We produce 200 simulated sample panels of dimension $N = 200, T = 200$. For each simulated sample, we estimate Γ under the two identification conditions Θ_{X} and Θ_{Y}. Figure 4 reports the histograms of the estimation errors and overlay them with the theoretical distributions for comparison. Given the data generating process, the theoretical distributions of estimation errors are approximated by the asymptotic distributions given in Theorem 3.[38]

The first panel reports estimation error $\widehat{\Gamma}(\Theta_{\text{X}}) - \Gamma^0(\Theta_{\text{X}})$. It corresponds to Theorem 3.a, or Arrow A in Figure 3. The four entries at the top are empty, because the corresponding four entries of Γ are pinned down by the identification condition and do not need to be estimated. The second panel corresponds to Theorem 3.b, or Arrow B. It reports $\widehat{\Gamma}(\Theta_{\text{Y}}) - \Gamma^0(\Theta_{\text{Y}})$. Note that while there are K^2 more distributions presented on the right, the two normalizations have exactly the same degrees of

[37] We generate $c_{i,t}$ with ex-ante i.i.d. means, so that each individual's time-series process is non-ergodic. This is deliberate so that $c_{i,t}$ admits the flexible property allowed by stochastic panels and resembles real-world instrument data.

[38] The required population moments, $\Omega^{cc}, \Omega^{cef}, \mathbb{V}^{[3]}$ etc., are calculated by large sample Monte Carlo. In the process of calculating these population quantities via Monte Carlo, we rotate the data generating process ex ante according to the required identification assumption IA. For example, f_t^0 needs to be inversely rotated when Γ^0 is normalized from $\Gamma^0(\Theta_{\text{Y}}^0)$ to $\Gamma^0(\Theta_{\text{X}})$, resulting in a different value for Ω^{cef}.

Figure 4: Γ Estimation Errors — Simulated v.s. Asymptotic Approximation

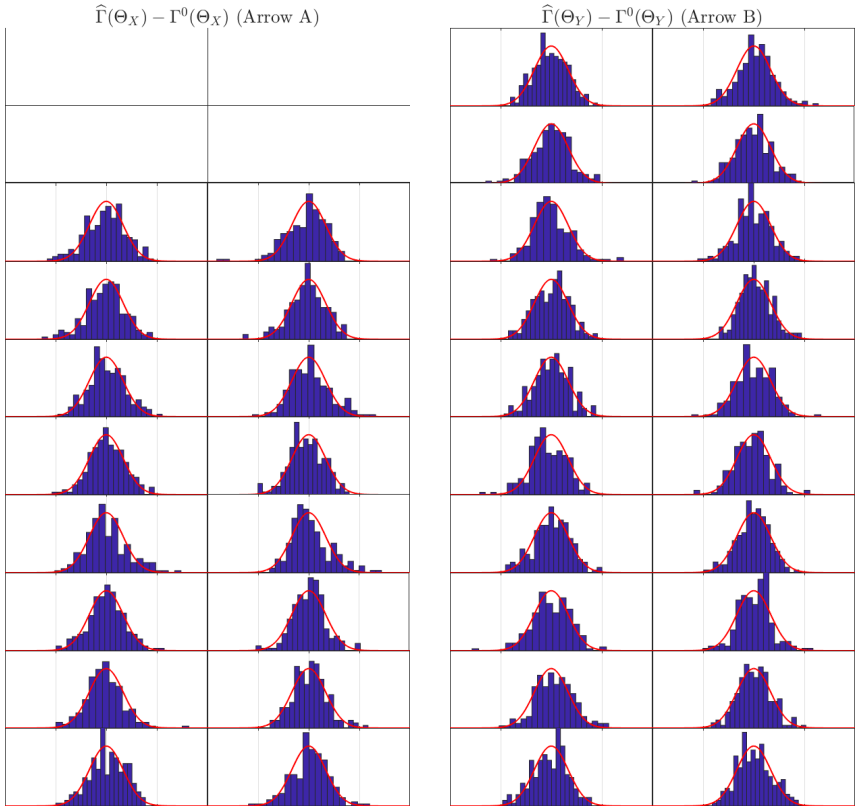

Note: This figure reports the small sample distributions of Γ estimation errors under the two example normalization cases. We conduct 200 simulations with sample dimensions $N = 200, T = 200$. The left panel reports the distribution of $\widehat{\Gamma}(\Theta_X) - \Gamma^0(\Theta_X)$ (Arrow A). The right panel reports the distribution of $\widehat{\Gamma}(\Theta_Y) - \Gamma^0(\Theta_Y)$ (Arrow B). Each subplot corresponds to one element in the $L \times K$ (10×2) matrix of Γ. Each histogram plots the simulated estimation errors, which is overlaid with the asymptotic distributions from Theorem 3 as finite sample approximations. The horizontal axis range is ±6 theoretical standard deviations, the tick marks are at ±3 theoretical standard deviations. The vertical axes are probability density for the bell curves or frequency density for the bars.

freedom. In other words, the top four distributions on the right duplicate information in the distributions plotted below them.

In all cases, the simulated distributions are centered around zero and match the theoretical distributions well. For some entries, we observe some skewness and tail heaviness. These are due to the small sample size and relatively large error variance in the generating process. In untabulated simulations with $N = 1000, T = 1000$, the asymptotics more-fully kick in and the distributions become visually indistinguishable from a normal. Hence, the simulation results suggest that even with panels of only

moderate size, our asymptotic approximations are accurate.

8 Applications

This section describes two empirical applications of IPCA to demonstrate its broad usefulness for analyzing economic data. The first is an application to international macroeconomics, where IPCA makes it easy analyze many nations' evolving relationships to global business cycles using country-level instruments. The second application builds on KPS and uses IPCA to analyze a dynamic model of asset risk and expected returns.

8.1 International Macroeconomics

Country-level macroeconomic fluctuations are globally connected (Backus et al., 1992). Using a static state-space model, Gregory et al. (1997) use maximum likelihood to document this for the G7 countries. Likewise, Kose et al. (2003) use a static state-space model estimated with Bayesian methods to disentangle global from regional and country-specific growth factors for a panel of countries over 30 years. Recently Kose et al. (2012) (henceforth KOP) used data from the World Development Indicators and estimated their static state-space model for a panel of countries before and after 1985 in order to analyze the convergence or decoupling of global business cycles. In essence, they ask: have countries' relationships to global growth changed as the countries themselves have evolved? This question is ideally suited for investigation with IPCA.

We use IPCA to analyze the global factor structure in GDP growth using data from the World Development Indicators database. We include as many countries as possible from the "industrial/developed" and "emerging" country groups studied by KOP. After reasonable data filters on indicators and countries, which we detail in the Appendix E, we are left with 45 countries. Within this sample there are nine variables that are available for most countries, so we use these as our instruments. The first two instruments are the import and export share of GDP—natural indicators of a country's economic connectedness with the rest of the world. Next we use the proportion of GDP relative to world GDP to measure the nation's relative size. We account for dynamics in capital intensity using gross capital formation, and we use popula-